# Gd$_3$N@C$_{84}$(OH)$_x$: A New Egg-Shaped Metallofullerene Magnetic Resonance Imaging Contrast Agent

Jianyuan Zhang,[†,‡] Youqing Ye,[†,‡] Ying Chen,[‡] Christopher Pregot,[‡] Tinghui Li,[†,‡]
Sharavanan Balasubramaniam,[§] David B. Hobart,[‡] Yafen Zhang,[‡] Sungsool Wi,[‡,Δ] Richey M. Davis,[§]
Louis A. Madsen,[‡] John R. Morris,[‡] Stephen M. LaConte,[†] Gordon T. Yee,*[,‡] and Harry C. Dorn*[,†,‡]

[†]Virginia Tech Carilion Research Institute, Roanoke, VA, 24016, United States
[‡]Department of Chemistry, Virginia Polytechnic Institute and State University, Blacksburg, Virginia, 24061 United States
[§]Department of Chemical Engineering, Virginia Polytechnic Institute and State University, Blacksburg, Virginia 24061, United States

**S** *Supporting Information*

**ABSTRACT:** Water-soluble derivatives of gadolinium-containing metallofullerenes have been considered to be excellent candidates for new magnetic resonance imaging (MRI) contrast agents because of their high relaxivity and characteristic encapsulation of the lanthanide ions (Gd$^{3+}$), preventing their release into the bioenvironment. The trimetallic nitride template endohedral metallofullerenes (TNT EMFs) have further advantages of high stability, high relative yield, and encapsulation of three Gd$^{3+}$ ions per molecule as illustrated by the previously reported nearly spherical, Gd$_3$N@$I_h$-C$_{80}$. In this study, we report the preparation and functionalization of a



lower-symmetry EMF, Gd$_3$N@$C_s$-C$_{84}$, with a pentalene (fused pentagons) motif and an egg-shaped structure. The Gd$_3$N@C$_{84}$ derivative exhibits a higher $^1$H MR relaxivity compared to that of the Gd$_3$N@C$_{80}$ derivative synthesized the same way, at low (0.47 T), medium (1.4 T), and high (9.4 T) magnetic fields. The Gd$_3$N@$C_s$-C$_{84}$ derivative exhibits a higher hydroxyl content and aggregate size, as confirmed by X-ray photoelectron spectroscopy (XPS) and dynamic light scattering (DLS) experiments, which could be the main reasons for the higher relaxivity.
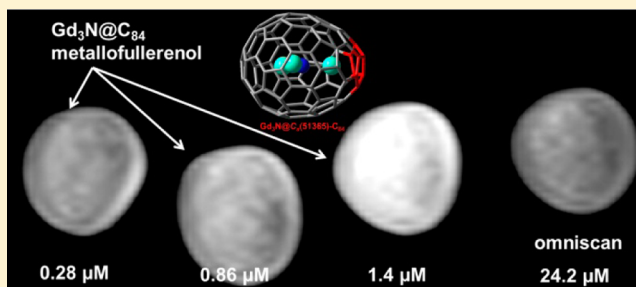
## INTRODUCTION

Gadolinium is an especially important element for medical diagnostics that is midway in the periodic progression of the lanthanide elements. The Gd$^{3+}$ ion with a half-filled 4f subshell (7 unpaired electrons) provides appealing paramagnetic properties with a relatively long electron spin−lattice time ($T_{1e}$) and has been widely applied in clinical magnetic resonance imaging (MRI) contrast agents.[1] In addition, various forms of Gd$^{3+}$ ion are key components for imaging purpose in the development of many theranostic nanomedicines.[2−5] In the search for next-generation MRI contrast agents, gadolinium metallofullerene derivatives are very promising materials. They confine the toxic Gd$^{3+}$ ions inside an inert yet robust carbon cage to preclude release, and exhibit 10−40 times higher proton relaxivity than commercial contrast agents[6] and in certain cases much longer retention in a mice model of glioma brain tumors.[7]

Early research on water-soluble derivatives of gadolinium metallofullerenes ("gadofullerenes") was pioneered by the Shinohara[6,8] and Wilson[9−11] groups and focused on mono-metal gadofullerenes, namely, Gd@C$_{82}$ and Gd@C$_{60}$. More recently, attention has focused on the trimetallic nitride template endohedral metallofullerenes (TNT EMFs).[12,13] Specifically, many water-soluble derivatives of Gd$_3$N@$I_h$-C$_{80}$

and Gd-containing mixed-metal TNT EMFs have been synthesized and tested as MRI contrast agents.[3,7,14−18] Distinct advantages of the TNT EMFs are their higher yields and up to three (as opposed to one) Gd$^{3+}$ ions inside a single fullerene cage. The research on TNT EMF-based contrast agents is limited to $I_h$-C$_{80}$ cage derivatives, even though other TNT EMF members have very different symmetry and shape[13] that may affect their relaxation behavior. For example, the pentalene-containing Gd$_3$N@$C_s$(51365)-C$_{84}$ (referred as "Gd$_3$N@C$_{84}$" in the rest of this paper since it is the only reported Gd$_3$NC$_{84}$ isomer) has an elipsoidal egg-shape,[19] in direct contrast to spherical Gd$_3$N@$I_h$-C$_{80}$[20] (Figure 1). Several other important structural features are very different between the two TNT EMFs. First, Gd$_3$N@$I_h$-C$_{80}$ has a pyramidal Gd$_3$N cluster, whereas Gd$_3$N@C$_{84}$ has a planar cluster. Second, on the basis of the results of a corresponding $^{89}$Y NMR study of diamagnetic Y$_3$N@$I_h$-C$_{80}$ and Y$_3$N@$C_s$(51365)-C$_{84}$,[21] Gd$_3$N@$I_h$-C$_{80}$ should exhibit isotropic motion of the (Gd$_3$N)$^{6+}$ cluster, whereas, Gd$_3$N@C$_{84}$ should exhibit restricted motion because of stronger association of one Gd atom to the pentalene motif. Third, the strong Gd−pentalene interaction provides a

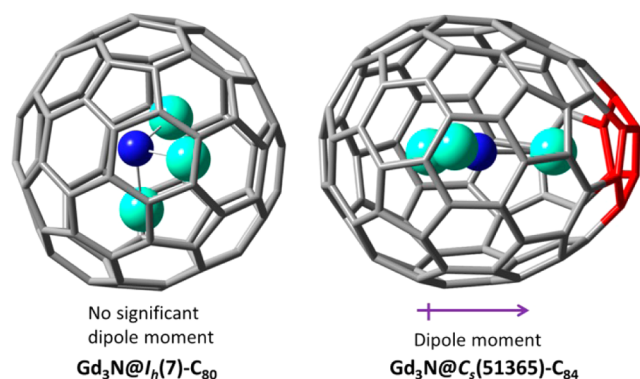**Figure 1.** Structures of $Gd_3N@I_h(7)\text{-}C_{80}$ (left) and $Gd_3N@C_s(51365)\text{-}C_{84}$ (right, pentalene unit shown in red).

significantly enhanced dipole moment for $Gd_3N@C_{84}$.[22] All of these differences may lead to different properties of their derivatives that could significantly alter MRI contrast efficiencies. Herein, we present new results for $Gd_3N@C_{84}$[19] and the corresponding water-soluble functionalized $Gd_3N@C_{84}(OH)_x$ directly compared with its $Gd_3N@C_{80}$ counterpart as a potential new MRI contrast agent.

## ■ EXPERIMENTAL SECTION

**Synthesis and Isolation of $Gd_3N@I_h(7)\text{-}C_{80}$ and $Gd_3N@C_s(51365)\text{-}C_{84}$.** LUNA Innovations provided the Gd metallofullerene soot utilizing previously reported procedures.[19,23] The resulting soot was extracted with xylene, and the solution was treated with cyclopentadiene-functionalized silica[24] with a "stir and filter approach"[25] for quick removal of empty-cage fullerenes. The filtrate containing Gd metallofullerenes was subjected to multistage high performance liquid chromatography (HPLC), which yielded purified $Gd_3N@I_h(7)\text{-}C_{80}$ and $Gd_3N@C_s(51365)\text{-}C_{84}$ Figure S1 in (Supporting Information [SI]).

**Synthesis of the Gd Metallofullerenols.** The functionalization of Gd TNT EMF (Scheme 1) was performed following the procedure

**Scheme 1. Functionalization of Gd TNT EMFs**
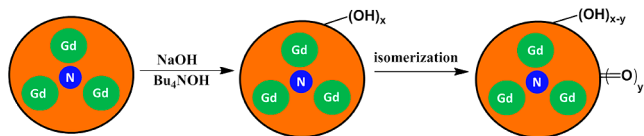


reported by Shinohara et al.[6] Briefly, to toluene solutions containing $Gd_3N@C_{80}$ (~1.0 mg) or $Gd_3N@C_{84}$ (~0.6 mg) were added 2 mL of 50 wt % NaOH solution and 2 drops of tetrabutyl ammonium hydroxide, and the mixtures were stirred at room temperature for 15 min. After the precipitation of a brown sludge, the toluene was removed by careful decantation. Then 10 mL more water was added to each reaction flask, and the resulting mixtures were stirred overnight to give light-brown aqueous solutions. Dilute hydrochloric acid was added dropwise to adjust the pH of the solutions to neutral. Then the each solution was placed in a cellulose dialysis bag (MWCO = 500) for a 7-day dialysis (water changed every 24 h) to give the water solutions of the corresponding Gd TNT EMF. Although the reaction aims to introduce hydroxyl groups, some carbonyl groups can be generated on the cage due to isomerization.

**SQUID Measurements of the Gd TNT EMF Samples.** The SQUID measurements were performed in a sample holder as previously reported.[26] For both $Gd_3N@C_{80}$ and $Gd_3N@C_{84}$, the dry metallofullerene powders were placed inside modified 5 mm NMR tubes. The magnetization was measured in a temperature range of 5−300 K at intervals of 5 K in a field of 5000 G. The sample size for $Gd_3N@C_{80}$ was 12.40 mg, and for $Gd_3N@C_{84}$ was 1.00 mg.

The experimental molar magnetic susceptibility ($\chi$) values contain three factors:

$$\chi_{obs} = \chi + \chi_d + \text{TIP} \tag{1}$$

in which $\chi_d$ is a small negative contribution from intrinsic diamagnetism of the material and the sample holder. In the data for $Gd_3N@C_{80}$ and $Gd_3N@C_{84}$ (Figure S2a,b in SI), the contribution due to the fullerene cage (paired electrons) is relatively small, as previously observed in a study of $Sc_3N@C_{80}$ and $Lu_3N@C_{80}$,[27] as well as our qualitative investigation of a mixture of $Lu_3N@C_{80}$ and $C_{60}$ (Figure S2C in SI) which has less than 1% magnetization compared to the Gd metallofullerene samples of same mass. The rest of the diamagnetic contribution is corrected by an empty-tube control experiment. TIP is a correction term that empirically accounts for the temperature independent paramagnetism (TIP) as has been previously observed.[27,28] The TIP term was empirically determined by fitting the susceptibility to the Curie−Weiss law

$$\chi^{-1} = \frac{T - \theta}{C} \tag{2}$$

in which $T$ is the temperature, $C$ is the material specific Curie constant, and $\theta$ is the Curie temperature. The Curie−Weiss law should be well obeyed for a half-filled shell ion. In other words, this procedure is equivalent to assuming that $\mu_B = (\sqrt{8\chi T})$ should asymptotically approach a constant value in the high-temperature limit where any interactions between the spins should be negligible.

**Relaxivity Measurement for the Metallofullerenols.** NMR relaxation measurements were performed on a Bruker Minispec mq20 (0.47 T) and mq60 (1.41 T) analyzers as well as a Bruker Avance III 400 MHz (9.4 T) wide bore spectrometer equipped with an MIC 400 W1/S2 probe and 5 mm $^1$H coil. The spin−lattice relaxation time $T_1$ was measured by the inversion−recovery method. The spin−spin relaxation time $T_2$ was measured by using an incremented echo-train CPMG pulse sequence. Errors in $T_1$ and $T_2$ values are generally less than ±2%. The concentration range for $Gd_3N@C_{80}$ metallofullerenols was 0.51−2.5 μM, and the concentration range for $Gd_3N@C_{84}$ metallofullerenols was 0.28−1.4 μM. A clinical Siemens Magnetom Trio MRI scanner was used to obtain the data for Figure 6.

## ■ RESULTS

**Chromatographic Separation of $Gd_3N@C_{80}$ and $Gd_3N@C_{84}$.** After chemical removal of the empty-cage fullerenes, the Gd-containing EMFs were loaded onto a pentabromobenzyl (PBB) column to give seven major fractions (Figure 2a).[23] The major components of each fraction are $Gd_2@C_{79}N$, $Gd_3N@I_h(7)\text{-}C_{80}$, $Gd_3N@C_s(39663)\text{-}C_{82}$, $Gd_3N@C_s(51365)\text{-}C_{84}$, $Gd_3N@D_3(19)\text{-}C_{86}$, $Gd_3N@D_2(35)\text{-}C_{88}$, and $Gd_2C_2@D_3(85)\text{-}C_{92}$, respectively. As seen in Figure 2a, $Gd_3N@C_{84}$ is the second most abundant Gd-EMF component, second only to $Gd_3N@C_{80}$. The chromatograms of purified Gd TNT EMFs on a pyrenylethyl (PYE) column are shown in Figure 2b. As previously reported, the retention time of EMFs increases with the size of metallofullerene cages and with increasing dipole moment. As a result, the egg-shaped $Gd_3N@C_{84}$ with a significant dipole moment possesses an elongated retention time relative to its cage size (Figure 2b). This result is consistent with a previously reported study where TNT EMFs with the pentalene motif have significantly longer retention times.[22]

**SQUID measurement of the magnetic moment for $Gd_3N@C_{80}$ and $Gd_3N@C_{84}$.** Although MR relaxivity ($r_1$, $r_2$) depends on a number of factors, a key factor is the effective magnetic moment ($\mu_{eff}$) *vide infra*. The magnetization vs temperature plot for $Gd_3N@C_{80}$ and $Gd_3N@C_{84}$ are shown in Figure S2. The effective moment values can be calculated from the equation below.
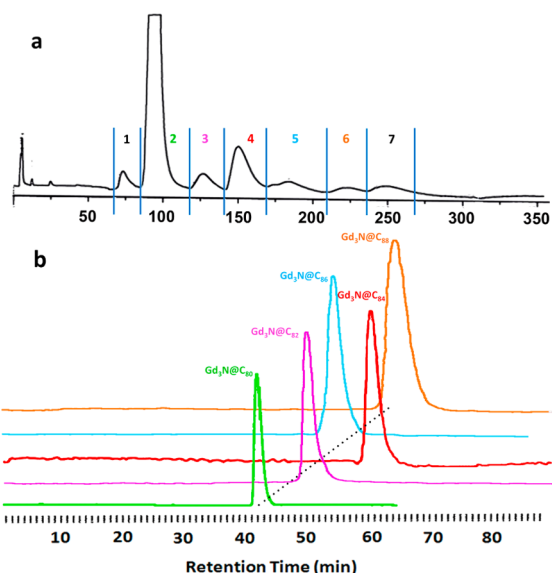
**Figure 2.** HPLC chromatograms of Gd-containing EMFs. (a) Mixture of Gd EMFs after chemical removal of empty-cage fullerenes on a PBB column (1.0 in. diameter) with toluene as eluent at 24 mL/min. (b) Isolated Gd TNT EMF members on PYE column (0.5 in. diameter) with toluene as eluent at 2 mL/min.

$$\mu_{\text{eff}} = (3k/N)^{1/2}(\chi T)^{1/2} = [g^2 s(s + 1)]^{1/2}\mu_B \qquad (3)$$

The obtained effective magnetic moment vs temperature plots are shown in Figures 3.

The $\mu_{\text{eff}}$ values for $Gd_3N@C_{80}$ and $Gd_3N@C_{84}$ are determined to be 10.8 $\mu_B$, and 11.5 $\mu_B$, at room temperature). The TIP for $Gd_3N@C_{80}$ is 0.0095 emu$^1$ mol$^{-1}$, and for $Gd_3N@C_{84}$ it is 0.23 emu$^1$ mol$^{-1}$. The larger number for $Gd_3N@C_{84}$ (probably due to the less than ideal sample size, 1.00 mg),



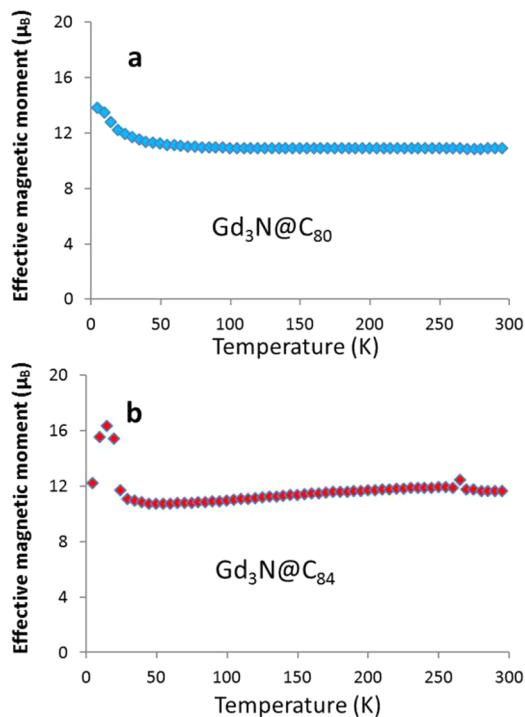**Figure 3.** Effective magnetic moment vs temperature plots for (a) $Gd_3N@C_{80}$ and (b) $Gd_3N@C_{84}$.

prevents further detailed quantitative comparison between the magnetic moments of $Gd_3N@C_{80}$ and $Gd_3N@C_{84}$; however, we note that qualitatively the two molecules have very similar magnetic behavior. They both show ferromagnetic coupling at low temperature which is consistent with a recent report.[29] What is surprising about our data is that the effective moment is well below the expected value of 13.7 $\mu_B$, which is calculated for three uncoupled spin-only $Gd^{3+}$ ions. Previously, other researchers observed similar results for $Gd_3N@C_{80}$ and ascribed the discrepancy to an unknown impurity and partly to an inaccurate mass.[28] Also, for monometallic fullerene $Gd@C_{82}$, the effective moment was determined in two independent measurements to be 6.9 $\mu_B$,[30,31] which is lower than that of the free $Gd^{3+}$. Shinohara proposed 1) crystal-field splitting of the metal orbital momentum states caused by the carbon cage and 2) the hybridization of the $4f$ orbital from the metal and the $\pi$ orbital from the carbon cage as possible reasons for this observation. For TNT EMFs antiferromagnetic interaction among the three $Gd^{3+}$ ions[32] is also a possibility. We will delve further into this anomalous result in future studies.

**Functionalization and Characterization of TNT EMFs.** EMFs require functionalization with hydrophilic groups in order to achieve sufficient water solubility, which is a prerequisite for aqueous MRI contrast agents. Among various choices, introduction of hydroxyl groups directly onto fullerene cages is the simplest and most effective approach. Hydroxyls enable proton exchange at minimum distance from the paramagnetic center (the encapsulated $Gd^{3+}$) thus maximizing proton relaxivity, which is proportional to the inverse six-power of this distance ($r_1 \propto r^{-6}$).[1] Also, hydroxyl groups on the cage can facilitate the formation of hydrogen-bonded aggregates that increase the correlation time of the contrast agent. Therefore, even when other hydrophilic groups, such as polyethylene glycol (PEG) chains and carboxyl groups, could also enhance water solubility, hydroxyl groups are still introduced onto the cage.[7,14,17] Additionally, we note that metallofullerenol (hydroxylated metallofullerene) was studied first as a metallofullerene-based MRI contrast agent candidate.[6]

$Gd_3N@C_{80}$ and $Gd_3N@C_{84}$ were converted to the corresponding metallofullerenols with the procedure used for $Gd@C_{82}$.[6] Since the paramagnetism of gadofullerenes precludes NMR characterization, a parallel reaction was performed on $^{13}C$-enriched $Y_3N@C_{80}$ for an independent solid-state $^{13}C$ NMR study (Figure S2, SI). The $Y_3N@C_{80}$ sample was obtained from a $^{13}C$ enriched synthesis of yttrium metallofullerenes as previously reported.[33] After functionalization, the $^{13}C$ NMR signals of pristine $Y_3N@C_{80}$ disappeared from the region of 135−150 ppm, suggesting the destruction of the extended conjugated system. Consistent with this observation, the UV−vis-NIR spectra of $Gd_3N@C_{80}$ metallofullerenol and $Gd_3N@C_{84}$ metallofullerenol exhibit decreased conjugation features in comparison with the corresponding parent EMFs (Figure 4b, c), confirming the loss of extended aromaticity. Although the reaction was intended to introduce hydroxyl groups, the existence of carbonyl groups resulting from rearrangements is confirmed by the $^{13}C$ NMR of the $Y_3N@C_{80}$ metallofullerenol (Figure S2, SI) as well as by FT-IR and XPS spectra of the $Gd_3N@C_{80}$ and $Gd_3N@C_{84}$ metallofullerenols (Figure 4a,d,e). In the FT-IR spectra of $Gd_3N@C_{80}$ and $Gd_3N@C_{84}$ metallofullerenols (Figure 4a), the carbonyl content is reflected by the intensity of the C=O peaks around 1700 cm$^{-1}$, as well as the C−H peaks at 2880−3000 cm$^{-1}$ associated to the keto−enol type isomerization, and

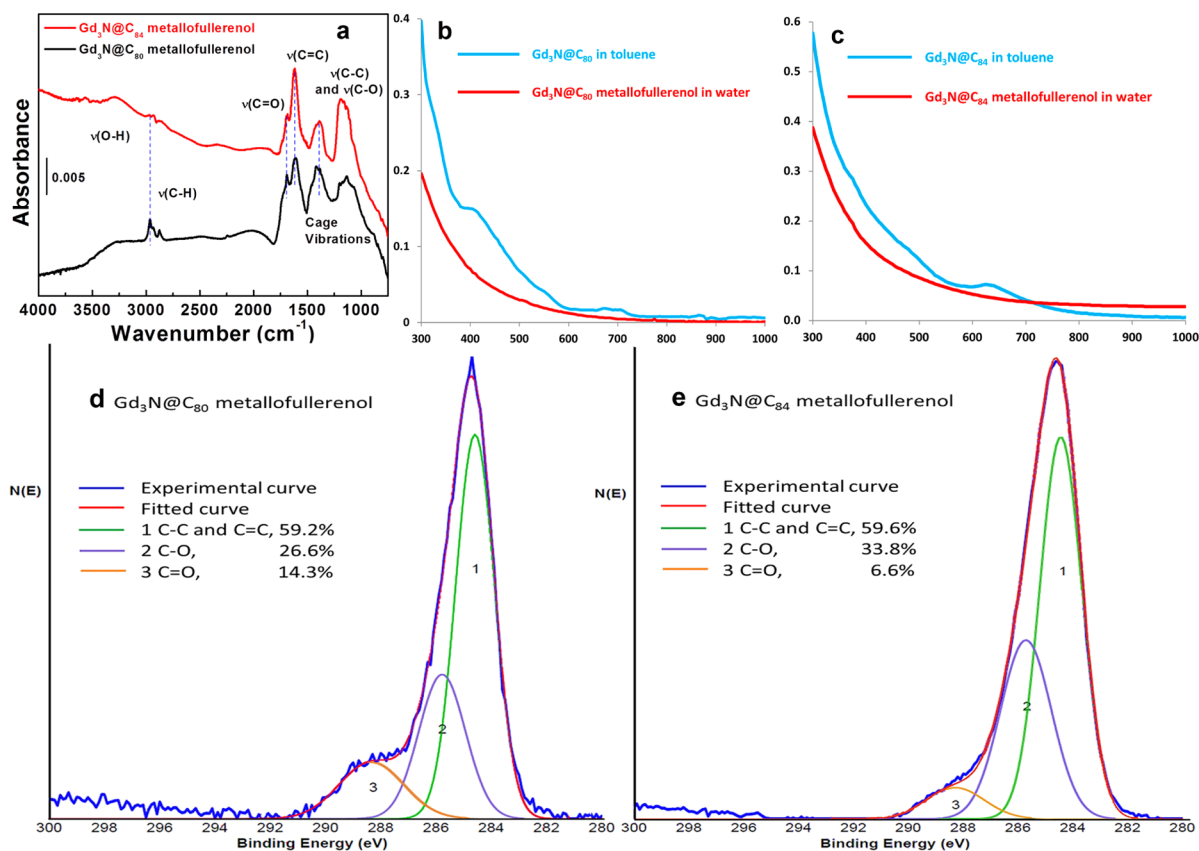**Figure 4.** Characterization of the $Gd_3N@C_{80}$ and $Gd_3N@C_{84}$ metallofullerenols. (a) FT-IR spectra for the $Gd_3N@C_{80}$ and $Gd_3N@C_{84}$ metallofullerenols. (b) UV−vis−NIR spectra for $Gd_3N@C_{80}$ before and after functionalization. (c) UV−vis-NIR spectra for $Gd_3N@C_{84}$ before and after functionalization. (d) XPS for the $Gd_3N@C_{80}$ metallofullerenol. (e) XPS for the $Gd_3N@C_{84}$ metallofullerenol.

the intensity of these peaks suggest the $Gd_3N@C_{84}$ metallofullerenol has lower carbonyl content. Furthermore, XPS is a well-established method to investigate the composition of fullerenols.[7,34−36] XPS data for $Gd_3N@C_{80}$ and $Gd_3N@C_{84}$ fullerenols were fitted using three peaks (Figure 4d,e): the C−C bond (284.5 eV), the C−O single bond (285.7 eV) and the C=O double bond (288.3 eV). In both cases about 40% of the carbon atoms were functionalized with oxygen; however, consistent with the FT-IR results, a clear difference was shown for the carbonyl content. The estimated formula for $Gd_3N@C_{80}$ metallofullerenol is $Gd_3N@C_{80}O_{11}(OH)_{21}$, and that for $Gd_3N@C_{84}$ metallofullerenol is $Gd_3N@C_{84}O_6(OH)_{28}$. The N 1s signals form the encapsulated nitrogen atoms in the EMF cages were also observed, as shown in Figure S4, SI.

**Dynamic Light Scattering on Trimetallic Nitride Metallofullerenols.** Water-soluble metallofullerene derivatives form aggregates in water, the size of which has a decisive role in their relaxivity.[37] Dynamic light scattering experiments were performed to investigate the hydrodynamic size of the aggregates formed by the trimetallic nitride metallofullerenols, and the results are shown in Figure 5. Each metallofullerenol had two different stages of aggregation. The $Gd_3N@I_h$-$C_{80}$ metallofullerenol showed two unresolved peaks (seen as one asymmetric peak) with a mean radius of 125 nm, which is similar to the carboxylated and hydroxylated derivative[7] and short-PEG chain attached derivative[17] of $Gd_3N@I_h$-$C_{80}$. Meanwhile, the $Gd_3N@C_{84}$ metallofullerenol showed a well-resolved bimodal distribution. A small peak was centered at 9.5 nm, while the large peak showed a mean radius of 179 nm, which is considerably larger than the counterpart aggregates of
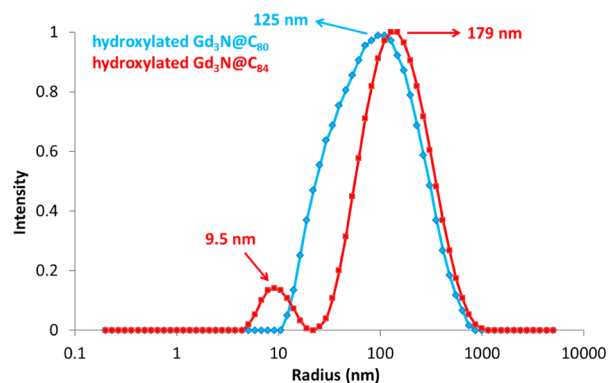


**Figure 5.** Hydrodynamic size distribution of metallofullerenol derivatives of $Gd_3N@I_h$-$C_{80}$ and $Gd_3N@C_3$-$C_{84}$.

metallofullerenol $Gd_3N@I_h$-$C_{80}$. The separate two stages of aggregation for hydroxylated $Gd_3N@C_{84}$ highly resemble the cases of polyethylene glycol (PEG) functionalized $Gd_3N@C_{80}$,[17] in which the longer PEG chain led to higher amounts of small aggregates. Therefore, the resolved peak for lower aggregate may be related to the less spherical shape of $Gd_3N@C_{84}$. It is possible to study the ratio between aggregated and free EMF derivatives in detail by NMR probes.[38]

**Relaxivity of the Trimetallic Nitride Metallofullerenols.** The ability of contrast agents to enhance MRI contrast is evaluated by relaxivity, which is defined by the equation:

**Table 1. Relaxivity Values for the $Gd_3N@C_{80}$ and $Gd_3N@C_{84}$ Metallofullerenols**

| metallofullerenol | 0.47 T, 298 K | | | 1.4 T, 310 K | | | 9.4 T, 298 K | | |
|---|---|---|---|---|---|---|---|---|---|
| | $r_1$ (mM$^{-1}$ s$^{-1}$) | $r_2$ (mM$^{-1}$ s$^{-1}$) | $r_2/r_1$ | $r_1$ (mM$^{-1}$ s$^{-1}$) | $r_2$ (mM$^{-1}$ s$^{-1}$) | $r_2/r_1$ | $r_1$ (mM$^{-1}$ s$^{-1}$) | $r_2$ (mM$^{-1}$s$^{-1}$) | $r_2/r_1$ |
| $Gd_3N@C_{80}O_{11}(OH)_{21}$ | 137 | 146 | 1.07 | 140 | 180 | 1.28 | 58 | 215 | 3.7 |
| $Gd_3N@C_{84}O_6(OH)_{28}$ | 170 | 232 | 1.36 | 173 | 238 | 1.38 | 63 | 320 | 5.1 |

$$\frac{1}{T_{i,\text{obs}}} = \frac{1}{T_{i,\text{H}_2\text{O}}} + \frac{1}{T_{i,\text{para}}} = \frac{1}{T_{i,\text{H}_2\text{O}}} + r_i[M] \quad i = 1, 2 \tag{4}$$

where $T_1$ and $T_2$ are longitudinal and transverse relaxation time, respectively. The relaxation rate (reciprocal of relaxation time) is determined by both diamagnetic (water) and paramagnetic (contrast agent) species, and the ratio of paramagnetic relaxation rate to the concentration is the relaxivity of the paramagnetic compound, which can be experimentally obtained by the slope of $(1/T_i)$ vs concentration of the paramagnetic contrast agents.

The relaxivity values of $Gd_3N@C_{80}$ metallofullerenol and $Gd_3N@C_{84}$ metallofullerenol were obtained at 0.47, 1.4, and 9.4 T magnetic fields, respectively. The results and the $r_2/r_1$ values are summarized in Table 1. Compared to the $\sim$4−6 mM$^{-1}$ s$^{-1}$ relaxivity for the commercial contrast agent Gd-DTPA (Magnevist), the relaxivity values for the trimetallic nitride metallofullerenols are significantly higher, and they did not change meaningfully from low to midfield strength, but significantly decreased at high field. The $Gd_3N@C_{84}$ metallofullerenol has considerably higher relaxivity values than $Gd_3N@C_{80}$ metallofullerenol, suggesting $Gd_3N@C_{84}$ is an excellent candidate as a new MRI contrast agent if it can be produced in large quantities.

***In vitro* MRI Study of Trimetallic Nitride Metallofullerenols.** For a visual confirmation of the efficiency of the trimetallic nitride metallofullerenols as contrast agents and a direct comparison between $Gd_3N@C_{80}$ and $Gd_3N@C_{84}$ metallofullerenols, $T_1$-weighted MR imaging was performed on their solutions in comparison with a commercial agent Omniscan (Figure 6) on a clinical MRI scanner. Significant signal enhancements were observed for both metallofullerenols in a concentration range of 0.3−3 $\mu$M (based on metallofullerenol molecule). The $r_1$ signal intensities (brightness) of the 0.51 $\mu$M $Gd_3N@C_{80}$ metallofullerenol (Figure 6a) and that of the 0.28 $\mu$M $Gd_3N@C_{84}$ metallofullerenol (Figure 6a) are qualitatively comparable, but are in 50−100-fold lower concentrations than needed for comparative contrast with Omniscan (24.2 $\mu$M) (Figure 6d,h). In each respective column of Figure 6, the $Gd_3N@C_{80}$ metallofullerenols (Figure 6a−c) have 1.8-fold higher concentrations compared to $Gd_3N@C_{84}$ metallofullerenols (Figure 6e−g), but still provide marginally lower contrast. In Figure 6b and 6g the metallofullerenols have similar concentration, but the image for $Gd_3N@C_{84}$ metallofullerenol is much brighter. These direct comparisons suggest that the $Gd_3N@C_{84}$ metallofullerenol prepared in this study is somewhat more effective as a contrast agent than $Gd_3N@C_{80}$ metallofullerenol in qualitative $T_1$-weighted MR imaging at clinical scanner magnetic field strengths.

## ■ DISCUSSION

The magnetic moment and proton relaxivity values are directly related. For $T_1$-weighted MRI, the contrast of the image can be represented by $1/T_1$, which is driven by dipole−dipole interactions and scalar contact (SC) interactions:
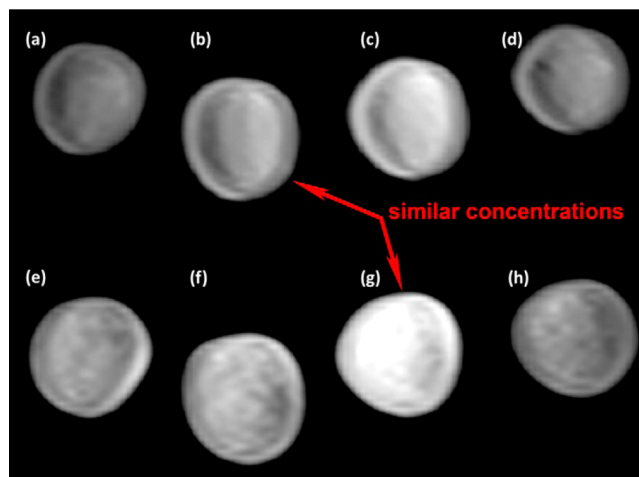


**Figure 6.** $T_1$-weighted MR images at 3 T (123 MHz) clinical scanner with Gd metallofullerenols as contrast agent (all samples in 5 mm tubes). Top line from left to right: (a) 0.51 $\mu$M $Gd_3N@C_{80}$ metallofullerenol, (b) 1.5 $\mu$M $Gd_3N@C_{80}$ metallofullerenol, (c) 2.5 $\mu$M $Gd_3N@C_{80}$ metallofullerenol, (d) 24.2 $\mu$M Omniscan. Bottom line from left to right: (e) 0.28 $\mu$M $Gd_3N@C_{84}$ metallofullerenol, (f) 0.86 $\mu$M $Gd_3N@C_{84}$ metallofullerenol, (g) 1.4 $\mu$M $Gd_3N@C_{84}$ metallofullerenol, (h) 24.2 $\mu$M Omniscan.

$$\frac{1}{T_1} = \frac{1}{T_1^{\text{DD}}} + \frac{1}{T_1^{\text{SC}}} \tag{5}$$

The two terms are determined by the equations below:[1]

$$\frac{1}{T_1^{\text{DD}}} = \frac{2}{15} \frac{\gamma_I^2 g^2 \mu_B^2 S(S+1)}{r^6} \left[ \frac{3\tau_{c1}}{(1 + \omega_I^2 3\tau_{c1}^2)} + \frac{7\tau_{c2}^2}{(1 + \omega_S^2 \tau_{c2}^2)} \right] \tag{6}$$

$$\frac{1}{T_1^{\text{SC}}} = \frac{2}{3} S(S+1) \left( \frac{A}{\hbar} \right)^2 \left[ \frac{\tau_e^2}{(1 + \omega_S^2 \tau_{e2}^2)} \right] \tag{7}$$

In the case of gadolinium EMFs, the dipole−dipole term is the dominant factor. From eqs 3 and 6, it is easily derived that

$$\mu_{\text{eff}}^2 \propto \frac{1}{T_1^{\text{DD}}}$$

The paramagnetism (effective magnetic moment) of the gadofullerenes originates from the seven unpaired $f$ electrons of the $Gd^{3+}$, and the functionalization only relates to the $s$ and $p$ orbitals of the carbon atoms on the fullerene cage. If this functionalization does not significantly change the effective magnetic moment of the encapsulated cluster ($Gd_3N$), the $r_1$ of the metallofullerenol should be proportional to the square of the $\mu_{\text{eff}}$ of the corresponding parent gadofullerene. The $\mu_{\text{eff}}$ of $Gd@C_{82}$ was previously determined to be 6.90 $\mu_B$.[30,31] On the basis of the $\mu_{\text{eff}}$ of $Gd_3N@C_{80}$ and $Gd_3N@C_{84}$, these
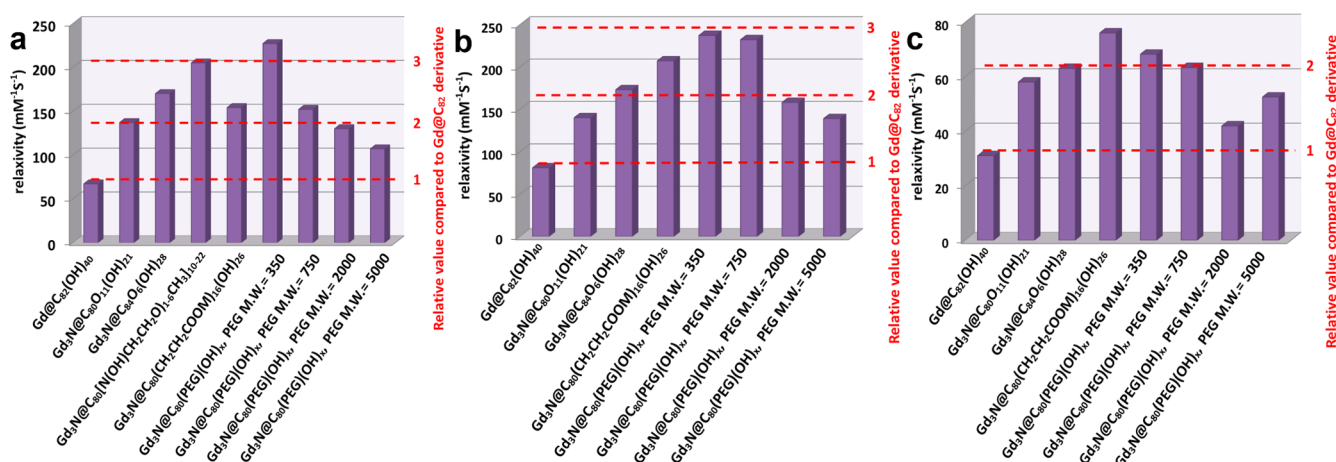
**Figure 7.** Summary of $r_1$ relaxivity values for $Gd@C_{82}$, $Gd_3N@C_{80}$, and $Gd_3N@C_{84}$ derivatives at (a) low magnetic field (0.35−0.47 T), (b) medium magnetic field (1.0−2.4 T) and (c) high magnetic field (4.7 T). In each panel, the left three columns represent the metallofullerene derivatives functionalized in the procedure described in current study. The data from previous reports cited in this figure are from refs 6, 7, 16, and 17

metallofullerenols should have ~2−3-fold higher $r_1$ compared to that of the same type of metallofullerenol, $Gd@C_{82}$.

Experimental $r_1$ values for gadofullerene derivatives $Gd@C_{82}$, $Gd_3N@C_{80}$, and $Gd_3N@C_{84}$ from the literature[6,7,16,17] and current work are shown in Figure 7 (values in Table S1 in the SI). As a semiquantitative overall trend, at respective field strengths, the $Gd_3N@C_{80}$ derivative has $r_1$ values of 1.8−2.0-fold higher than the $r_1$ of $Gd@C_{82}$ metallofullerenol for the same functionalization. Whereas, the $Gd_3N@C_{84}$ metallofullerenol has 2.0−2.4-fold higher values in comparison with those of $Gd@C_{82}$ for the same functionalization method. Furthermore, as a qualitative trend, a comparison of the $r_1$ values for the $Gd@C_{82}$, $Gd_3N@C_{80}$, and $Gd_3N@C_{84}$ derivatives versus other Gd TNT EMFs with different functionalization illustrate a factor of ~2−3 higher relaxivity relative to that of $Gd@C_{82}$ at all magnetic field strengths. These comparative results are in reasonably good agreement with the anticipated value from experimental $\mu_{eff}$ results, *vide supra*.

Another contributing factor for the significantly higher relaxivity of the $Gd_3N@C_{84}$ metallofullerenols is the lower carbonyl content. Previous fullerene hydroxylation showed that carbonyl groups are easier to form under acidic conditions;[39] however they can also form in lower amounts under basic or neutral conditions.[40] XPS data revealed that carbonyl formation is less favored for $Gd_3N@C_{84}$ than for $Gd_3N@C_{80}$, likely related to the low symmetry and special egg shape caused by the pentalene unit. One reaction mechanism accounting for this difference is related to the hopping of negative charges. Nucleophilic attack from a hydroxyl group creates a carbanionic site on the cage surface, which can be readily oxidized by oxygen.[41] The involvement of oxygen had been confirmed by an argon-protected reaction that led to very low yield.[40] Before oxidation, the negative charge can be dispersed over the fullerene cage via the π-conjugated system to form enolic groups, which are potential sources of carbonyl formation via enol-keto isomerization. An example of such a rearrangement is illustrated in Figure S5 in the SI. For $Gd_3N@C_{84}$ which has an ellipsoidal shape with enhanced dipole moment,[19,22] the electron density is unevenly distributed on the cage, and it is reasonable to expect the nucleophilic reaction sites are "crowded" on parts of the cage with lower electron density, rather than uniformly spread out as in the case of $Gd_3N@C_{80}$,

which is expected to lower the negative charge hopping and limit carbonyl formation.

The size of aggregates is also a key factor for the relaxivity by affecting the correlation time ($\tau_C$).[17] DLS data suggested that $Gd_3N@C_{84}$ metallofullerenol forms larger aggregates than that of $Gd_3N@I_h\text{-}C_{80}$ metallofullerenol, which is consistent with the relaxivity results. The difference in aggregation observed for the $Gd_3N@C_{84}$ metallofullerenol versus the $Gd_3N@C_{80}$ metallofullerenol could be the result of the special ellipsoidal shape (enhanced dipole moment) of the starting material and the higher hydroxyl content, facilitating greater intermolecular hydrogen bond formation. Moreover, the special shape and higher hydroxyl content can facilitate the $Gd_3N@C_{84}$ metallofullerenols to trap more water molecules in its aggregates, which could result in enhanced relaxivity.

In addition, the distance between the paramagnetic site (the $Gd^{3+}$) and the proton exchange site (the −OH) has an inverse sixth order contribution to the relaxivity.[1] It is possible that the fixed cluster in $Gd_3N@C_{84}$ directs the functionalization reaction to occur on the carbon atoms near the $Gd^{3+}$ ions, while the rotating cluster in the $Gd_3N@C_{80}$ has no such effect. Further detailed characterization of these derivatives is necessary to confirm this hypothesis.

## ■ CONCLUSION

We have investigated the magnetic moment of TNT EMF $Gd_3N@C_{80}$ and $Gd_3N@C_{84}$ and the $^1H$ relaxivity of their metallofullerenol derivatives. The two TNT EMFs have similar effective magnetic moments. The relaxivity of $Gd_3N@C_{84}$ metallofullerenol is significantly higher than the $Gd_3N@C_{80}$ metallofullerenol when both are synthesized under identical conditions. We suggest that the ellipsoidal shape and the pentalene motif of $Gd_3N@C_{84}$ system contributes to the difference in functionalization, aggregation, and relaxivity in comparison with those of the $Gd_3N@C_{80}$ system. With the increasing yield of EMFs, $Gd_3N@C_{84}$ and other pentalene-containing metallofullerenes could evolve as excellent candidates for next-generation MRI contrast and theranostic agents.

## ASSOCIATED CONTENT

**S** **Supporting Information**

HPLC and MS characterization of $Gd_3N@I_h$-$C_{80}$ and $Gd_3N@$ $C_s$-$C_{84}$, $^{13}C$ NMR of the $Y_3N@I_h$-$C_{80}$ metallofullerenol, IR spectra for both gadolinium metallofullerenols, proposed mechanism for isomerization of the metallofullerenols. This material is available free of charge via the Internet at http://pubs.acs.org.

## AUTHOR INFORMATION

**Corresponding Authors**
gyee@vt.edu
hdorn@vt.edu

**Present Address**
△National High Magnetic Field Laboratory, Tallahassee, FL 32310, United States.

**Notes**
The authors declare no competing financial interest.

## ACKNOWLEDGMENTS

## REFERENCES

(1) Caravan, P.; Ellison, J. J.; McMurry, T. J.; Lauffer, R. B. *Chem. Rev.* **1999**, *99*, 2293.

(2) Bryson, J. M.; Fichter, K. M.; Chu, W.-J.; Lee, J.-H.; Li, J.; Madsen, L. A.; McLendon, P. M.; Reineke, T. M. *Proc. Natl. Acad. Sci. U.S.A.* **2009**, *106*, 16913.

(3) Shultz, M. D.; Wilson, J. D.; Fuller, C. E.; Zhang, J.; Dorn, H. C.; Fatouros, P. P. *Radiology* **2011**, *261*, 136.

(4) Zhen, M.; Zheng, J.; Wang, Y.; Shu, C.; Gao, F.; Zou, J.; Pyykkö, I.; Wang, C. *Chem.—Eur. J.* **2013**, *19*, 14675.

(5) Kelkar, S. S.; Reineke, T. M. *Bioconjugate Chem.* **2011**, *22*, 1879.

(6) Mikawa, M.; Kato, H.; Okumura, M.; Narazaki, M.; Kanazawa, Y.; Miwa, N.; Shinohara, H. *Bioconjugate Chem.* **2001**, *12*, 510.

(7) Shu, C.; Corwin, F. D.; Zhang, J.; Chen, Z.; Reid, J. E.; Sun, M.; Xu, W.; Sim, J. H.; Wang, C.; Fatouros, P. P.; Esker, A. R.; Gibson, H. W.; Dorn, H. C. *Bioconjugate Chem.* **2009**, *20*, 1186.

(8) Kato, H.; Kanazawa, Y.; Okumura, M.; Taninaka, A.; Yokawa, T.; Shinohara, H. *J. Am. Chem. Soc.* **2003**, *125*, 4391.

(9) Bolskar, R. D.; Benedetto, A. F.; Husebo, L. O.; Price, R. E.; Jackson, E. F.; Wallace, S.; Wilson, L. J.; Alford, J. M. *J. Am. Chem. Soc.* **2003**, *125*, 5471.

(10) Tóth, É.; Bolskar, R. D.; Borel, A.; González, G.; Helm, L.; Merbach, A. E.; Sitharaman, B.; Wilson, L. J. *J. Am. Chem. Soc.* **2004**, *127*, 799.

(11) Sitharaman, B.; Bolskar, R. D.; Rusakova, I.; Wilson, L. J. *Nano Lett.* **2004**, *4*, 2373.

(12) Stevenson, S.; Rice, G.; Glass, T.; Harich, K.; Cromer, F.; Jordan, M. R.; Craft, J.; Hadju, E.; Bible, R.; Olmstead, M. M.; Maitra, K.; Fisher, A. J.; Balch, A. L.; Dorn, H. C. *Nature* **1999**, *401*, 55.

(13) Zhang, J.; Stevenson, S.; Dorn, H. C. *Acc. Chem. Res.* **2013**, *46*, 1548.

(14) Fatouros, P. P.; Corwin, F. D.; Chen, Z.-J.; Broaddus, W. C.; Tatum, J. L.; Kettenmann, B.; Ge, Z.; Gibson, H. W.; Russ, J. L.; Leonard, A. P.; Duchamp, J. C.; Dorn, H. C. *Radiology* **2006**, *240*, 756.

(15) Zhang, E.-Y.; Shu, C.-Y.; Feng, L.; Wang, C.-R. *J. Phys. Chem. B* **2007**, *111*, 14223.

(16) MacFarland, D. K.; Walker, K. L.; Lenk, R. P.; Wilson, S. R.; Kumar, K.; Kepley, C. L.; Garbow, J. R. *J. Med. Chem.* **2008**, *51*, 3681.

(17) Zhang, J.; Fatouros, P. P.; Shu, C.; Reid, J.; Owens, L. S.; Cai, T.; Gibson, H. W.; Long, G. L.; Corwin, F. D.; Chen, Z.-J.; Dorn, H. C. *Bioconjugate Chem.* **2010**, *21*, 610.

(18) Fatouros, P. P.; Shultz, M. D. *Nanomedicine* **2013**, *8*, 1853.

(19) Zuo, T.; Walker, K.; Olmstead, M. M.; Melin, F.; Holloway, B. C.; Echegoyen, L.; Dorn, H. C.; Chaur, M. N.; Chancellor, C. J.; Beavers, C. M.; Balch, A. L.; Athans, A. J. *Chem. Commun.* **2008**, 1067.

(20) Stevenson, S.; Phillips, J. P.; Reid, J. E.; Olmstead, M. M.; Rath, S. P.; Balch, A. L. *Chem. Commun.* **2004**, 2814.

(21) Fu, W.; Xu, L.; Azurmendi, H.; Ge, J.; Fuhrer, T.; Zuo, T.; Reid, J.; Shu, C.; Harich, K.; Dorn, H. C. *J. Am. Chem. Soc.* **2009**, *131*, 11762.

(22) Zhang, J.; Bearden, D. W.; Fuhrer, T.; Xu, L.; Fu, W.; Zuo, T.; Dorn, H. C. *J. Am. Chem. Soc.* **2013**, *135*, 3351.

(23) Fu, W.; Zhang, J.; Fuhrer, T.; Champion, H.; Furukawa, K.; Kato, T.; Mahaney, J. E.; Burke, B. G.; Williams, K. A.; Walker, K.; Dixon, C.; Ge, J.; Shu, C.; Harich, K.; Dorn, H. C. *J. Am. Chem. Soc.* **2011**, *133*, 9741.

(24) Ge, Z. X.; Duchamp, J. C.; Cai, T.; Gibson, H. W.; Dorn, H. C. *J. Am. Chem. Soc.* **2005**, *127*, 16292.

(25) Stevenson, S.; Harich, K.; Yu, H.; Stephen, R. R.; Heaps, D.; Coumbe, C.; Phillips, J. P. *J. Am. Chem. Soc.* **2006**, *128*, 8829.

(26) Sellers, S. P.; Korte, B. J.; Fitzgerald, J. P.; Reiff, W. M.; Yee, G. T. *J. Am. Chem. Soc.* **1998**, *120*, 4662.

(27) Smirnova, T. I.; Smirnov, A. I.; Chadwick, T. G.; Walker, K. L. *Chem. Phys. Lett.* **2008**, *453*, 233.

(28) Náfrádi, B.; Antal, Á.; Pásztor, Á.; Forró, L.; Kiss, L. F.; Fehér, T.; Kováts, É.; Pekker, S.; Jánossy, A. *J. Phys. Chem. Lett.* **2012**, *3*, 3291.

(29) Hermanns, C. F.; Bernien, M.; Krueger, A.; Schmidt, C.; Wasserroth, S. T.; Ahmadi, G.; Heinrich, B. W.; Schneider, M.; Brouwer, P. W.; Franke, K. J.; Weschke, E.; Kuch, W. *Phys. Rev. Lett.* **2013**, *111*.

(30) Funasaka, H.; Sakurai, K.; Oda, Y.; Yamamoto, K.; Takahashi, T. *Chem. Phys. Lett.* **1995**, *232*, 273.

(31) Kitaura, R.; Okimoto, H.; Shinohara, H.; Nakamura, T.; Osawa, H. *Phys. Rev. B* **2007**, *76*, 172409.

(32) Lu, J.; Sabirianov, R. F.; Mei, W. N.; Gao, Y.; Duan, C.-g.; Zeng, X. *J. Phys. Chem. B* **2006**, *110*, 23637.

(33) Zhang, J.; Fuhrer, T.; Fu, W.; Ge, J.; Bearden, D. W.; Dallas, J.; Duchamp, J.; Walker, K.; Champion, H.; Azurmendi, H.; Harich, K.; Dorn, H. C. *J. Am. Chem. Soc.* **2012**, *134*, 8487.

(34) Husebo, L. O.; Sitharaman, B.; Furukawa, K.; Kato, T.; Wilson, L. J. *J. Am. Chem. Soc.* **2004**, *126*, 12055.

(35) Shu, C. Y.; Gan, L. H.; Wang, C. R.; Pei, X. L.; Han, H. B. *Carbon* **2006**, *44*, 496.

(36) Shu, C.-Y.; Wang, C.-R.; Zhang, J.-F.; Gibson, H. W.; Dorn, H. C.; Corwin, F. D.; Fatouros, P. P.; Dennis, T. J. S. *Chem. Mater.* **2008**, *20*, 2106.

(37) Laus, S.; Sitharaman, B.; Tóth, É.; Bolskar, R. D.; Helm, L.; Asokan, S.; Wong, M. S.; Wilson, L. J.; Merbach, A. E. *J. Am. Chem. Soc.* **2005**, *127*, 9368.

(38) Wang, X.; Kelkar, S. S.; Hudson, A. G.; Moore, R. B.; Reineke, T. M.; Madsen, L. A. *ACS Macro Lett.* **2013**, *2*, 1038.

(39) Kato, H.; Suenaga, K.; Mikawa, M.; Okumura, M.; Miwa, N.; Yashiro, A.; Fujimura, H.; Mizuno, A.; Nishida, Y.; Kobayashi, K.; Shinohara, H. *Chem. Phys. Lett.* **2000**, *324*, 255.

(40) Li, J.; Takeuchi, A.; Ozawa, M.; Li, X. H.; Saigo, K.; Kitazawa, K. *J. Chem. Soc., Chem. Commun.* **1993**, 1784.

(41) Russell, G. A.; Bemis, A. G. *J. Am. Chem. Soc.* **1966**, *88*, 5491.